

Non-polar InGaN quantum dot emission with crystal-axis oriented linear polarization

Benjamin P. L. Reid,^{1, a)} Claudius Kocher,² Tongtong Zhu,³ Fabrice Oehler,³ Christopher C. S. Chan,² Rachel A. Oliver,³ and Robert A. Taylor²

¹⁾*Department of Physics, University of Oxford, Clarendon Laboratory, Oxford, OX1 3PU, UK*

²⁾*Department of Physics, University of Oxford, UK*

³⁾*Department of Materials Science and Metallurgy, University of Cambridge, UK*

(Dated: 21 April 2015)

Polarization sensitive photoluminescence is performed on single non-polar InGaN quantum dots. The studied InGaN quantum dots are found to have linearly polarized emission with a common polarization direction defined by the [0001] crystal axis. Around half of ~ 40 studied dots have a polarization degree of 1. For those lines with a polarization degree less than 1, we can resolve fine structure splittings between $-800\mu\text{eV}$ and $+800\mu\text{eV}$, with no clear correlation between fine structure splitting and emission energy.

^{a)}benjamin.reid@physics.ox.ac.uk

Semiconductor quantum dots (QDs) have been the subject of intense recent research due to their fundamental physical properties, and potential applications in quantum optoelectronic devices. In particular, optical quantum computing¹⁻³ and quantum cryptography^{4,5} require sources of polarized single photons^{6,7} and entangled photon pairs⁸.

Both electrically driven single qubit emitters^{9,10} and entangled photon pairs^{11,12} have been demonstrated in Group III-As QDs but the small confinement potential in these QDs limits their operation to cryogenic temperatures. Group III-N QDs offer a much deeper confinement potential and quantum confinement has been observed up to room temperature¹³⁻¹⁵. A complication in using these III-N QDs as two-level systems comes from the internal electric field present as a consequence of their wurtzite crystal structure. Recently however, exceptionally small QDs¹⁶ or growth on a non-polar crystal plane¹⁷ have been used to demonstrate coherently driven Rabi oscillations^{18,19}.

In this letter we investigate the polarization properties of non-polar InGaN quantum dots, which have been shown to have short lifetime transitions¹⁷, high thermal stability of the exciton transition²⁰, and high energy states decoupled from the QD wetting layer¹⁹. We observe many QD spectral lines with a polarization degree (defined by the normalized differential of the intensities of each fine-structure component) of 1 and no corresponding fine-structure split line, suggesting that one fine-structure component of the transition has a much greater oscillator strength than the other. Other observed QD spectral lines reveal a fine-structure splitting (FSS) between two orthogonal polarization components with an FSS less than the typical linewidth of the QD transitions (~ 1 meV). All QD lines have a common polarization angle ($\pm 10^\circ$) which we show to correspond to the $[0001]$ crystal axis. The high degree of polarization and common polarization axis represent significant advantages over other blue-UV QD emitters²¹⁻²⁴ in the context of building a source of polarized single photons suitable for applications in optical quantum computation and quantum cryptography.

The non-polar InGaN QD samples were grown by metal-organic vapour phase epitaxy in a Thomas-Swan 6×2 in. close-coupled showerhead reactor on r -plane $(1\bar{1}02)$ Al_2O_3 substrates with ammonia, trimethylindium, and trimethylgallium as the precursor gases. a -plane pseudo-substrates were prepared by epitaxial layer overgrowth as detailed elsewhere^{25,26}. An InGaN epilayer was grown at 695°C and annealed at the same temperature in a N_2 atmosphere, replicating the modified droplet epitaxy approach used in the growth of c -plane InGaN QDs²⁷. After annealing, a capping layer of ~ 10 nm GaN is grown at the same tem-

perature, before another ~ 10 nm GaN growth is carried out at 1050°C in H_2 . The density of QDs was estimated at $1 \times 10^8 \text{ cm}^{-2}$ by cathodoluminescence.

A pattern of $1 \mu\text{m}$ diameter circular apertures in a metal mask was created using electron beam lithography and a chemical wet etch to ensure optical isolation of single QDs, with an average of ~ 1 QD per aperture.

The sample was mounted on a cold-finger within a continuous helium flow cryostat (Janis ST-500). A feedback loop temperature controller (Lakeshore 331) was used to ensure a stable temperature of 4.2 K . The excitation source was a picosecond pulsed Ti:Sapphire laser operating at 800 nm , which was focussed onto the sample using a $100\times$ achromatic-corrected IR objective with a numerical aperture of 0.5 . The spectral resolution of the laser ($\delta E = 1.3 \text{ meV}$) is small enough such that two-photon absorption above the InGaN band gap can be induced²⁸, a method which has been shown to increase the contrast between the luminescence from the QDs and that from the underlying non-continuous quantum well layer which is a consequence of the growth procedure^{17,27}. The emitted photoluminescence (PL) is collected by the same IR objective, imaged onto a $50 \mu\text{m}$ slit, and dispersed by a 1200 lines/mm grating in a 0.3 m spectrometer (Shamrock 303i) and detected by a Peltier cooled Si-based charge-coupled device. Polarization dependent PL spectra were taken by placing a Glan-Thompson polarizer and a $\lambda/2$ waveplate into the collection path. For every rotation of the polarizer through an angle α from vertical, the half waveplate is rotated by $\alpha/2$ to ensure vertically polarized light enters the spectrometer, meaning the maximum signal intensity possible is recorded.

Figure 1 shows an example of a 100% linearly polarized transition at $\sim 486 \text{ nm}$ (within the signal to noise of the measurement system). The axis of the linear polarizer has been set so that a polarizer angle of 0° corresponds to the maximum intensity of the QD emission line. With the polarization axis orthogonal to that which obtains the maximum QD intensity, the luminescence is completely suppressed within the noise of the CCD. The wider features in the PL spectra in figure 1 correspond to emission from the discontinuous underlying quantum well layer (a consequence of the growth method), and can also appear to be suppressed at a polarizer angle of 90° as expected for the A-exciton emission from an InGaN quantum well²⁹. Fluctuations in dimension and composition of the QW layer lead to different polarization dependences however, as well as wider emissions on both at both higher and lower energy than the QDs.

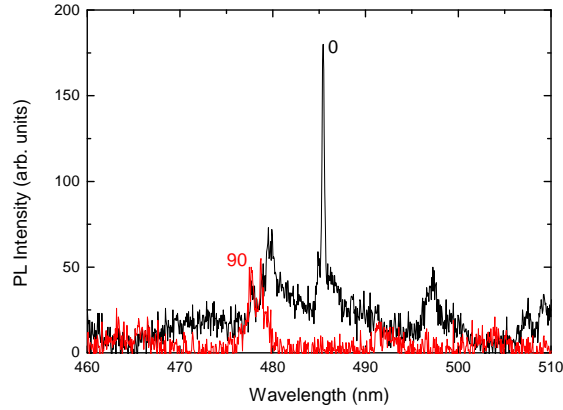


FIG. 1. PL emission intensity from a studied QD emitting at ~ 486 nm at two orthogonal polariser angles. The emission is completely suppressed at a polariser angle of 90° within the noise of the CCD.

Other quantum dots measured showed polarizer angles corresponding to the maximum QD intensity which match with the angle set by the QD in figure 1 within $\pm 10^\circ$ with no exceptions in a sample of 40 studied QDs. This is in direct contrast with results obtained in other III-N QD systems²¹, as well as polar InGaN QDs²².

In figure 2 we show the emission intensity of the QD luminescence from figure 1 as a function of polarizer angle. The QD luminescence intensity follows the expected behaviour for linear polarized light, with good agreement between the data and a fit of the data to the function $I(\theta) = I_{\max} \cos^2(\theta)$, where I_{\max} corresponds to the emission intensity at a polarizer angle of zero. In figure 2 (a) an optical microscope image shows striations visible in the surface of the sample, which correspond to the $[0001]$ crystal direction as confirmed during the growth process. Since these striations can be seen by focussing white light into our confocal microscope setup during the PL experiments, we can use them to relate the common polarization axis observed to a crystal axis, and find it corresponds to the $[0001]$ axis.

We interpret the direction of the polarization axis as follows: The polar nature of the $[0001]$ -direction (c -direction) in InN/GaN means that a QD formed with the c -axis in its basal plane (the case for a non-polar QD) will be strained along the c -direction, leading to an asymmetry of the confinement potential in the QD. This modification of the confinement potential causes the exciton to preferentially oscillate along the c -direction, thereby emitting

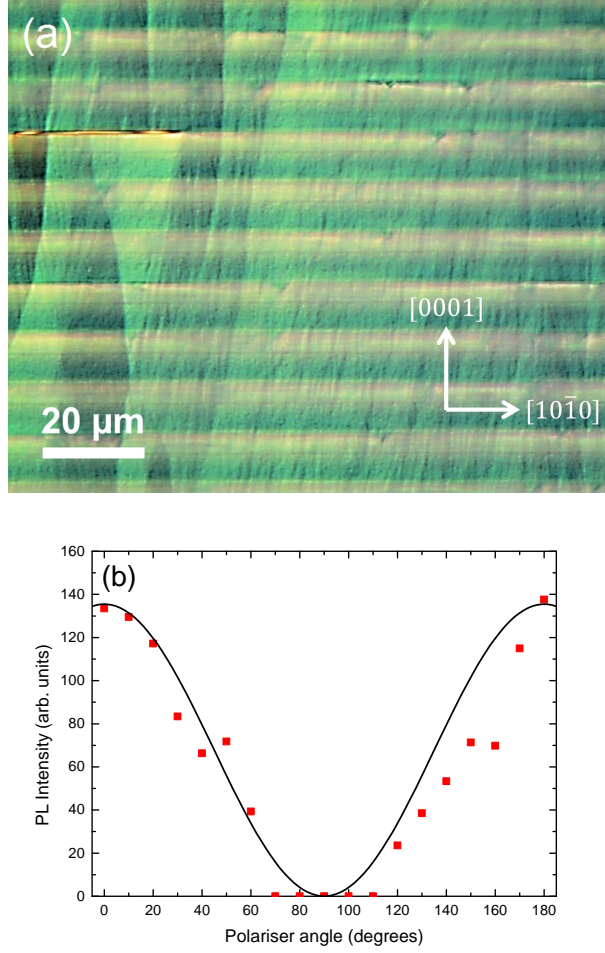


FIG. 2. (a) Optical microscope image showing surface striations which run along the [0001] crystal direction, and SiO₂ strips running along the [10 $\bar{1}$ 0] direction. The striations allow us to orient the polarisation axis to be along [0001] at a polariser angle of 0°. (b) PL emission intensity (red points) against polarizer angle for a studied QD. The emission line has a polarization degree of 1 and can be well fitted by $I(\theta) = I_{\max} \cos^2(\theta)$ (black line).

linear polarized light with a polarization axis corresponding to the c -axis. In the case where a QD line exhibits a polarization degree of less than 1, we do not see a random polarization direction, instead the emission remains predominately polarized along the c -direction, with a small component in the perpendicular direction. We can therefore postulate that an additional asymmetry in either QD shape or position of the indium atoms gives rise to an out-of-plane asymmetry in the QD confinement potential in addition to the in-plane asymmetry associated with the strain along the c -direction.

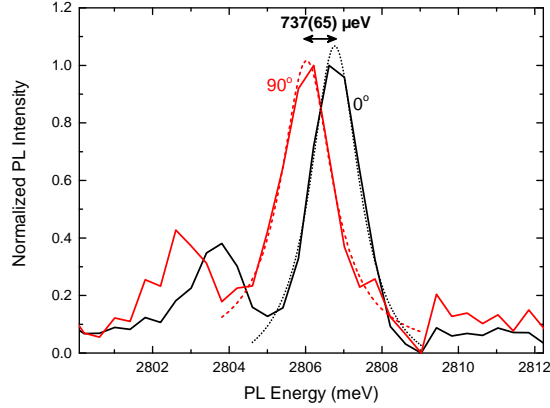


FIG. 3. Normalized PL emission intensity from a QD at two orthogonal polariser angles. The dotted lines represent Lorentzian fits of the data which enable us to extract a value for the fine structure splitting of $-737(65) \mu\text{eV}$. Each spectrum was integrated for a period of 5 minutes to rule out any effect of spectral drift on the data.

In the case of an asymmetry which is both in-plane (caused by the strain inherent in the crystal structure) and out-of-plane (caused by asymmetry in the shape and/or indium composition of the QD), we expect to measure a polarization degree < 1 and to therefore resolve the fine-structure splitting of the bright-exciton state. In figure 3 we show spectra taken at orthogonal polarizer angles, integrated for 5 minutes. The long integration time is selected to reduce any error in the QD energy caused by spectral drift of the exciton energy over time^{30,31}. We can resolve a FSS for the QD in figure 3 of $-737(65) \mu\text{eV}$, with the higher energy brighter in intensity by a factor ~ 10 . Such a value for the FSS is similar to that reported for polar InGa_N QDs²², but much smaller than the $2 - 7 \text{ meV}$ reported for GaN QDs²¹. We also observe cases where the emission is brighter at lower energy, indicating a positive fine structure splitting. With both positive and negative values observed there could be the possibility of tuning the fine structure splitting towards zero for applications as a source of entangled photons³².

In figure 4, we present the measured FSS values for 14 QDs which had strong enough signal to noise ratios between the fine-structure split emission lines. The current data do not appear to show a clear correlation between emission energy and fine-structure splitting, in contrast to the case for InAs QDs³³. We attribute this to the fact that several parameters

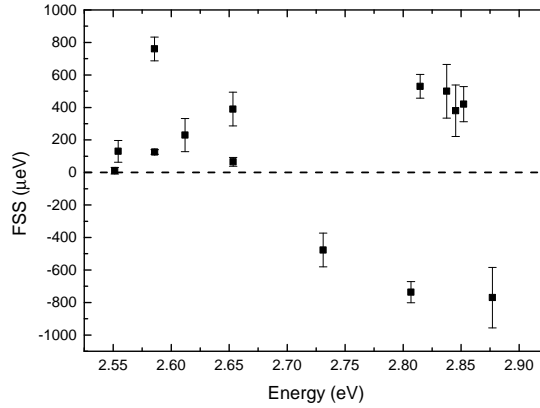


FIG. 4. Fine structure splittings measured for 14 of the studied quantum dots plotted against emission energy. No discernible correlation can be observed, in contrast to previous reports on InAs and GaN QDs.

such as QD size, indium content, and internal electric field can affect the QD emission energy. A much better understanding of the variation in size, shape and indium content of the non-polar QDs (possibly through transmission electron microscopy and PL on the same QDs) will be required to attempt to tune the FSS to zero with any regularity.

In conclusion, we have performed polarization dependent photoluminescence on single non-polar InGa_N quantum dots. All measured QDs show linear polarization along an axis corresponding to the [0001] crystal axis, many with a polarization degree of 1, a consequence of the strain inherent in the wurtzite crystal structure. This strain induced asymmetry causes one fine-structure component of the emission to be suppressed, meaning only photons polarized along the [0001] crystal direction are detected. For those emission lines with polarization degree < 1 , a fine structure splitting between $-800 \mu\text{eV}$ and $+800 \mu\text{eV}$ can be observed, with no clear correlation between emission energy and fine structure splitting. These results suggest non-polar InGa_N QDs represent an interesting avenue for research into polarized single photon sources and entangled photon sources.

REFERENCES

- ¹E. Knill, R. Laflamme, and G. J. Milburn, *Nature* **409**, 46 (2001).
- ²J. L. O’Brien, *Science* **318**, 1567 (2007).

- ³D. Loss and D. P. DiVincenzo, Phys. Rev. A **57**, 120 (1998).
- ⁴C. Kurtsiefer, P. Zarda, M. Halder, H. Weinfurter, P. M. Gorman, P. R. Tapster, and J. G. Rarity, Nature **419**, 450 (2002).
- ⁵C.-Z. Peng, T. Yang, X.-H. Bao, J. Zhang, X.-M. Jin, F.-Y. Feng, B. Yang, J. Yang, J. Yin, Q. Zhang, N. Li, B.-L. Tian, and J.-W. Pan, Phys. Rev. Lett. **94**, 150501 (2005).
- ⁶A. Muller, J. Breguet, and N. Gisin, EPL (Europhysics Letters) **23**, 383 (1993).
- ⁷P. Michler, A. Kiraz, C. Becher, W. V. Schoenfeld, P. M. Petroff, L. Zhang, E. Hu, and A. Imamoglu, Science **290**, 2282 (2000).
- ⁸T. Jennewein, C. Simon, G. Weihs, H. Weinfurter, and A. Zeilinger, Phys. Rev. Lett. **84**, 4729 (2000).
- ⁹A. Lochmann, E. Stock, O. Schulz, F. Hopfer, D. Bimberg, V. Haisler, A. Toropov, A. Bakarov, and A. Kalagin, Electronics Letters **42**, 774 (2006).
- ¹⁰T. Miyazawa, S. Okumura, S. Hirose, K. Takemoto, M. Takatsu, T. Usuki, N. Yokoyama, and Y. Arakawa, Japanese Journal of Applied Physics **47**, 2880 (2008).
- ¹¹N. Akopian, N. H. Lindner, E. Poem, Y. Berlatzky, J. Avron, D. Gershoni, B. D. Gerardot, and P. M. Petroff, Phys. Rev. Lett. **96**, 130501 (2006).
- ¹²J. E. Avron, G. Bisker, D. Gershoni, N. H. Lindner, E. A. Meirom, and R. J. Warburton, Phys. Rev. Lett. **100**, 120501 (2008).
- ¹³M. J. Holmes, K. Choi, S. Kako, M. Arita, and Y. Arakawa, Nano Letters **14**, 982 (2014), pMID: 24422516.
- ¹⁴S. Deshpande, A. Das, and P. Bhattacharya, Applied Physics Letters **102**, 161114 (2013).
- ¹⁵S. Kako, C. Santori, K. Hoshino, S. Gotzinger, Y. Yamamoto, and Y. Arakawa, Nat Mater **5**, 887 (2006).
- ¹⁶M. Choi, K. Arita, S. Kako, and Y. Arakawa, J. Cryst. Growth **370**, 328 (2013).
- ¹⁷T. Zhu, F. Oehler, B. P. L. Reid, R. M. Emery, R. A. Taylor, M. J. Kappers, and R. A. Oliver, Applied Physics Letters **102**, 251905 (2013).
- ¹⁸M. Holmes, S. Kako, K. Choi, P. Podemski, M. Arita, and Y. Arakawa, Phys. Rev. Lett. **111**, 057401 (2013).
- ¹⁹B. P. L. Reid, C. Kocher, T. Zhu, F. Oehler, R. Emery, C. C. S. Chan, R. A. Oliver, and R. A. Taylor, Applied Physics Letters **104**, 263108 (2014).
- ²⁰B. P. L. Reid, T. Zhu, C. C. S. Chan, C. Kocher, F. Oehler, R. Emery, M. J. Kappers, R. A. Oliver, and R. A. Taylor, physica status solidi (c) **11**, 702 (2014).

- ²¹C. Kindel, S. Kako, T. Kawano, H. Oishi, Y. Arakawa, G. Hönig, M. Winkelkemper, A. Schliwa, A. Hoffmann, and D. Bimberg, *Phys. Rev. B* **81**, 241309 (2010).
- ²²S. Amloy, Y. T. Chen, K. F. Karlsson, K. H. Chen, H. C. Hsu, C. L. Hsiao, L. C. Chen, and P. O. Holtz, *Phys. Rev. B* **83**, 201307 (2011).
- ²³S. Amloy, K. F. Karlsson, T. G. Andersson, and P. O. Holtz, *Applied Physics Letters* **100**, 021901 (2012).
- ²⁴K. F. Karlsson, S. Amloy, Y. T. Chen, K. H. Chen, H. C. Hsu, C. L. Hsiao, L. C. Chen, and P. O. Holtz, *Physica B: Condensed Matter* **407**, 1553 (2012).
- ²⁵C. Johnston, M. Kappers, M. Moram, J. Hollander, and C. Humphreys, *Journal of Crystal Growth* **311**, 3295 (2009).
- ²⁶M. Häberlen, T. J. Badcock, M. A. Moram, J. L. Hollander, M. J. Kappers, P. Dawson, C. J. Humphreys, and R. A. Oliver, *Journal of Applied Physics* **108**, 033523 (2010).
- ²⁷R. A. Oliver, G. A. D. Briggs, M. J. Kappers, C. J. Humphreys, S. Yasin, J. H. Rice, J. D. Smith, and R. A. Taylor, *Applied Physics Letters* **83**, 755 (2003).
- ²⁸A. F. Jarjour, A. M. Green, T. J. Parker, R. A. Taylor, R. A. Oliver, G. A. D. Briggs, M. J. Kappers, C. J. Humphreys, R. W. Martin, and I. M. Watson, *Physica E: Low-dimensional Systems and Nanostructures* **32**, 119 (2006).
- ²⁹T. J. Badcock, P. Dawson, M. J. Kappers, C. McAleese, J. L. Hollander, C. F. Johnston, D. V. Sridhara Rao, A. M. Sanchez, and C. J. Humphreys, *physica status solidi (c)* **6**, S523 (2009).
- ³⁰J. H. Rice, J. W. Robinson, A. Jarjour, R. A. Taylor, R. A. Oliver, G. A. D. Briggs, M. J. Kappers, and C. J. Humphreys, *Applied Physics Letters* **84**, 4110 (2004).
- ³¹B. P. L. Reid, T. Zhu, T. J. Puchtler, L. J. Fletcher, C. C. S. Chan, R. A. Oliver, and R. A. Taylor, *Japanese Journal of Applied Physics* **52**, 08JE01 (2013).
- ³²R. Trotta, E. Zallo, C. Ortix, P. Atkinson, J. D. Plunhof, J. van den Brink, A. Rastelli, and O. G. Schmidt, *Phys. Rev. Lett.* **109**, 147401 (2012).
- ³³R. J. Young, R. M. Stevenson, A. J. Shields, P. Atkinson, K. Cooper, D. A. Ritchie, K. M. Groom, A. I. Tartakovskii, and M. S. Skolnick, *Phys. Rev. B* **72**, 113305 (2005).